

Infrared spectroscopy of the hole subbands on Si

F. Martelli, C. Mazuré, and F. Koch

Physik-Department, Technische Universität München, D-8046 Garching, Federal Republic of Germany

(Received 5 March 1984)

We study the intersubband resonant absorption of holes on the major symmetry planes of Si using radiation polarized both perpendicular and parallel to the surface. The energies of absorption maxima are compared with those obtained from inelastic-light-scattering experiments.

I. INTRODUCTION

Infrared subband absorption spectroscopy is a well-known tool for the investigation of the energy-band structure of a surface charge layer. A large number of materials have been studied to date. In particular, electrons on Si, as a model case, have received a lot of attention. Electron spectra have been studied, both theoretically and experimentally, for all the major surface orientations, as a function of temperature up to 300 K, for densities N_s to $\sim 2 \times 10^{13} \text{ cm}^{-2}$ and using ir polarization both parallel and perpendicular to the sample surface. A review of such work is found in Ref. 1.

By contrast relatively little has been done for surface hole layers on Si, because the complicated valence-band structure precludes easy and straightforward interpretation of the spectra. Along with the electron signals, hole intersubband absorption on (100) Si was first reported in Refs. 2 and 3. Kamgar⁴ extended such experiments to (110) and (111) planes for a few laser energies and $N_s \sim 10^{12} \text{ cm}^{-2}$.

Only recently a concerted effort has been made to explore the Si hole subbands spectroscopically. Claessen⁵ showed that holes can be excited using parallel polarization. The possibility of parallel excitation is utilized in the recent Fourier transformation spectroscopy experiments of Wieck *et al.*^{6,7} The present work makes use of fixed frequency lasers and a grating spectrometer. We provide a comparison of data in both the parallel and perpendicular excitation modes. Measurements are made over a more complete energy range (7–80 meV) and to larger N_s values ($\leq 18 \times 10^{12} \text{ cm}^{-2}$) than in Ref. 7. Observations as a function of temperature up to ~ 200 K are included. The infrared absorption data are compared with the recently completed, inelastic-light-scattering results of Baumgartner *et al.*⁸ obtained in our laboratory and on the same samples.

II. EXPERIMENTAL NOTES

We employ the spectrometers and techniques developed in previous experiments.^{3,9} Energies $\hbar\omega \leq 30.2$ meV are the discrete lines of a molecular gas, far-infrared laser. Higher excitation energies are obtained from a global source and grating monochromator. Measurements are made in simple transmission for parallel excitation, whereas for perpendicular polarization the strip transmission line geometry is employed. The grating spectrometer

optics precludes the strip line technique, so that only parallel-excited data are available at the higher energies.

For the measurement the source energy is fixed and the surface carrier density N_s is swept through the resonance. Spectra are obtained as a derivative of the transmitted intensity T by modulating the surface electric field (dT/dV_G or dT/dN_s). The change ΔT is measured using on-off chopping of the surface layer charge. These methods are described adequately in previous work.³

The samples are metal-oxide-semiconductor capacitors with gate areas $6 \times 8 \text{ mm}^2$ prepared from n -type Si wafers of the desired orientation. We have deliberately chosen n -type ($N_D \sim 2 \times 10^{15} \text{ cm}^{-3}$) material in order to have the possibility to examine both hole inversion and quasi-accumulation layers. Quasi-accumulation conditions apply when the sample is illuminated with above-band-gap radiation. The illumination intensity is raised sufficiently to assure that the absorption line has the position and shape appropriate for accumulation. Parallel and perpendicular polarization data are obtained on the same sample making use of side-by-side thin Ni-Cr ($\sim 100 \text{ \AA}$) and thick Al ($\sim 2000 \text{ \AA}$) gates.

III. THEORY NOTES: BASIC IDEAS FOR HOLE-SUBBAND SPECTROSCOPY

Hole subbands for inversion layers (n -type Si, $N_D = 1 \times 10^{15} \text{ cm}^{-3}$) have been calculated by different authors^{8,10,11} in the self-consistent-potential (Hartree) approximation. The results differ substantially in detail. The inclusion of many-body effects as in Ref. 12 significantly alters the subband energy values.

The disagreement between the various theories makes a comparison of the infrared spectra with calculations difficult. More than that, the neglect of specific features of the infrared excitation experiments makes it questionable. The depolarization shift as well as the final-state interaction (the exciton shift), are not included in the theoretical description. Moreover, theory gives a strong dependence of the intersubband transition energy and spin splitting on the electron momentum $\hbar k_{\parallel}$ along the surface. The absorption signal will be an inhomogeneously broadened line, whose maximum is the weighted resultant of density of states and matrix element effects summed over the distribution of occupied k_{\parallel} states.

The k_{\parallel} sum is expected to depend on the polarization of the exciting radiation. The usual, allowed subband excitation is the mode for which the infrared electric field is

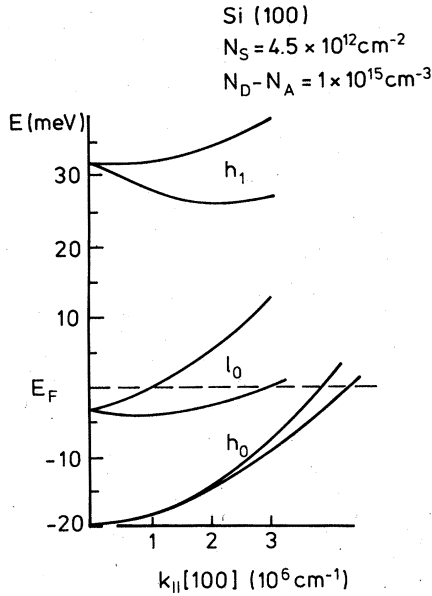


FIG. 1. Hole subbands vs $k_{||}$ in the [100] direction according to Bangert (Refs. 8 and 11). Subbands h and l are derived from the heavy and light hole bands in bulk Si. The subbands are spin split for $k \neq 0$. Note that the energy separations of the subbands depend on $k_{||}$ and the spin splitting.

perpendicular to the surface. This is the only mode in which subband electrons in the parabolic conduction band of (100) Si can be excited. Parallel excitation is possible whenever the dispersion relation of the carriers involves a coupling of the perpendicular and parallel motions. One such case that is discussed at length in the literature^{13,14} is the case of the nonparabolic conduction band on narrow-gap semiconductors. Another one is the tilted-ellipsoid geometry of (110) and (111) Si electrons.^{9,15,16} Parallel excitation of the Si holes is possible because of the warping of the constant energy surfaces. Specifically, the dispersion of the bulk Si energy bands contains terms of the type $k_{||}^2 k_{\perp}^2$ under the square root. Thus it appears that for states with $k_{||} \neq 0$ there exists the possibility of $||$ excitation. The weighting of the $||$ excitation will be a function of $k_{||}$ and will lead to a different sum over the distribution of states than for \perp excitation.

We illustrate in Fig. 1, with a calculation of the subband structure taken from Ref. 11, some basic features of the hole subbands and their resonance excitation. The subbands are formed from the three volume bands at the Γ point of the Brillouin zone which are known as heavy holes (h), light holes (l), and spin-orbit-split holes (s). The l - h degeneracy is removed by the surface potential in the formation of the surface bands. The lowest bound state is h -like. It is labeled h_0 to designate the first of a series $n=0,1,2,\dots$, of h -like states. The next higher and partially filled subband is the l_0 subband. It is followed by h_1 . The energy scale (marked in meV in Fig. 1) is such that bands l , h , and s all participate in the formation of the surface-bound levels. As the l - h splitting at $k_{||}=0$ shows, the surface potential mixes the bands. The surface bands are spin split for $k_{||} \neq 0$ and vary nonpara-

bolically with $k_{||}$. Moreover, the pairs of levels between which transitions take place do not vary in the same way with $k_{||}$, so that their separation depends on $k_{||}$. The splitting and the dependence on $k_{||}$ differ with the orientation of $k_{||}$ in the plane.

The infrared absorption spectrum involves electric dipole transitions among the various states in Fig. 1. We must expect that because the bands are significantly hybridized, transitions are allowed to some degree between most pairs of occupied-empty states. A comparison of experiment and theory must account for this weighting of transition matrix elements in order to correctly describe the absorption structure and assign transitions.

The experimental observation of an absorption maximum serves as a characteristic of the spectrum. It is not simply linked with the separation at $k_{||}=0$ of a pair of the surface bands. The reader is cautioned about drawing conclusions hastily from the possible agreement of a measured energy with the calculations. We prefer not to make the comparison with the $k_{||}=0$ separations of the theory. The present experiments make use of an N_s sweep at fixed frequency and thus obtain a resonant absorption signal under conditions of changing occupancy of the $k_{||}$ states. For various reasons, this will influence the line shape and possibly the position of maximal absorption.

IV. RESULTS AND DISCUSSION

A. General features of the hole resonances

In Fig. 2 we show an example of electron and hole resonances in the perpendicular excitation mode. The upper curves are the transmission derivative (dT/dV_g) signals. The solid line is obtained with illumination of the sample and represents accumulation for both electrons and holes.

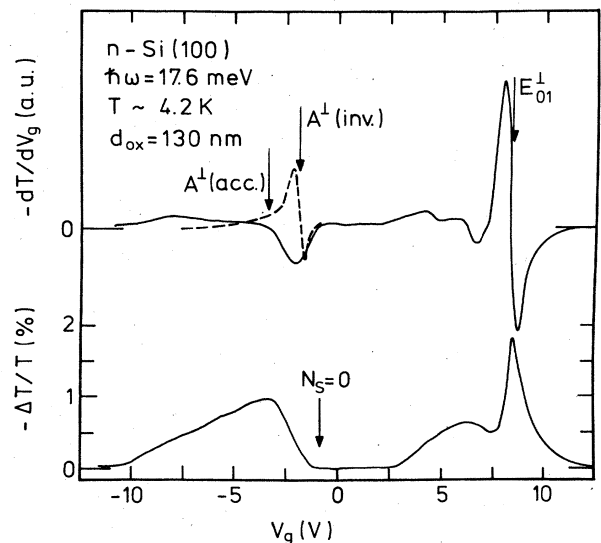


FIG. 2. Comparison of electron ($V_g > 0$) and hole ($V_g < 0$) resonances in the (100) plane of Si as observed in the \perp polarization mode. $A^+(\text{acc})$ marks the absorption maximum under quasiaccumulation conditions, $A^+(\text{inv})$ the corresponding inversion-layer case.

Under such conditions the $N_s=0$ marking applies for both types of carriers. The density scale is $1.65 \times 10^{11} \text{ cm}^{-2} \text{ V}^{-1}$.

The lower half of Fig. 2 gives the transmission change ΔT in terms of percent of T . Such data is obtained by on-off, square-wave modulation of the surface charge N_s starting at $N_s=0$. The ΔT magnitude depends on the dimensions of the strip line and the length of the sample.

Both the dT/dV_g and $\Delta T(V_g)$ curves make clear that the hole absorption line is strongly asymmetric and significantly broader than the electron signal. The only distinct feature of ΔT is a maximum which coincides with the $dT/dV_g=0$ marked as A^\perp in the figure. The broad, asymmetric ΔT curve is evidence for a resonance composed of a $k_{||}$ sum of transitions with different energy separations.

Labeling the hole resonance and assigning it to a particular transition is a problem. For the electrons, E_{01}^\perp represents the N_s value for which the resonance energy for transitions from the $n=0$ ground state to the $n=1$ level is $\hbar\omega$. The many transitions that are possible in the scheme of Fig. 1, in particular the $k_{||}$ dependence, precludes a straightforward assignment for the hole resonances. The observed resonance peak is a characteristic of the spectrum of transitions which extend over a range of excitation energies. We refer to the absorption maxima in an alphabetic sequence A, B, C , etc., denoting whether they are observed in parallel ($||$) or perpendicular (\perp) polarization with the corresponding superscript.

Marking the resonances in $||$ excitation spectra is complicated by the fact that they include a Drude-type background signal. The background is particularly noticeable at low energies. For the $||$ polarization spectra we subtract a background in the dT/dV_g curve and mark the resonance accordingly not at zero. The parallel spectra contain at low N_s an interface-impurity-dependent structure¹⁷ that must not be misinterpreted as a resonance.

To illustrate how sensitively the hole resonance at low N_s depends on the depletion field we show in the broken line of Fig. 2 the inversion-layer spectrum for the same sample. It is obtained as a dark sweep³ starting at -10 V . The capacitance indicates a depletion charge $N_{\text{dep}} = 2.7 \times 10^{11} \text{ cm}^{-2}$ under the conditions of the experiment. The $N_s=0$ for such a sweep is to the left of the marker. The resonance $A^\perp(\text{inv})$ occurs at a lower N_s value. The line is narrower and more symmetric than the accumulation layer case. We take this as evidence for a reduction of the inhomogeneous broadening that occurs when the occupancy of the $k_{||}$ states is reduced. The broadening with rising N_s is distinctly seen in experiments with fixed N_{dep} (Fig. 1 in Ref. 2).

B. Parallel versus perpendicular excitation

In the theory section we noted that parallel excitation is possible for states with $k_{||} \neq 0$. Signals with comparable amplitudes are generally found in $||$ and \perp excitation. For a broad line the absorption maximum can easily be shifted when the weighting of the individual contributions is changed by the polarization. There is in addition the depolarization effect that distinguishes \perp and $||$ excited

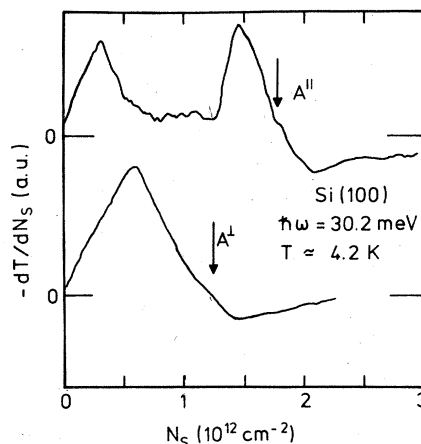


FIG. 3. Comparison of the $||$ and \perp excited A resonances in (100) Si (quasi accumulation). Note the impurity peak at low N_s in the $||$ mode (compare Ref. 17).

data. Typically electron resonances are depolarization shifted to $\sim 30\%$ higher $\hbar\omega$ in the \perp polarization mode.^{9,15}

Figure 3 shows the hole excitation spectra for (100) Si with $\hbar\omega=30.2 \text{ meV}$ in the two polarization modes. The arrows labeled $A^{||}$ and A^\perp mark the absorption maximum. As expected for the depolarization effect, the \perp excited resonance occurs at lower N_s . The $||$ excited spectrum in the upper curve of Fig. 3 has an additional peak at low N_s . This particular structure differs from sample to sample and is influenced by charged impurities (e.g., Na^+) at the interface. It does not shift with frequency like a subband resonance.¹⁷

The distinction between $||$ and \perp excited resonance positions is not so clear in the (110) plane. The $A^{||}$ and A^\perp signals in Fig. 4 have more nearly the same position. The overall line shape differs considerably. The $||$ polarization mode gives a low- N_s impurity absorption contribution

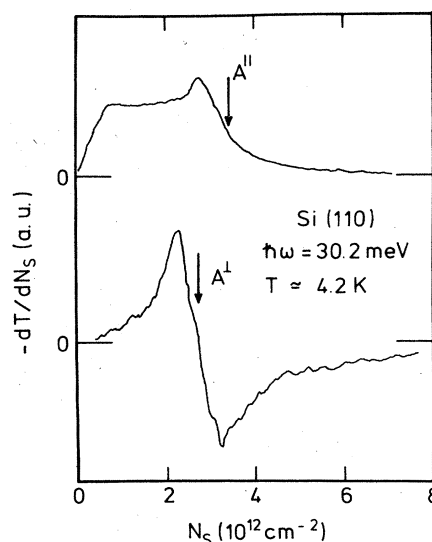


FIG. 4. Comparison of $A^{||}$ and A^\perp resonances in the (110) Si (quasi accumulation).

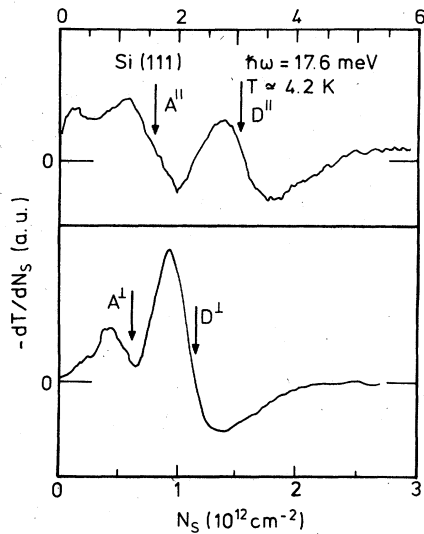


FIG. 5. Comparison of the resonances in the (111) plane with the two polarization modes. The splittings are unusually large in this plane (note the different scales).

similar to that in Fig. 3. The light scattering experiments also show the polarization splitting to be small for the (110) plane. In Ref. 8 the \parallel excited resonances actually lie at energies above those of \perp excitation. This is not the case for the infrared spectra. In Raman experiments the two excitation modes are observed in the light scattered with polarization parallel or perpendicular to that of the incident beam. They have been referred to as "single-particle" and "collective" modes, respectively.

In Fig. 5 we show the (111) plane spectra for a relatively low $\hbar\omega = 17.6$ meV. In this plane and energies below 40 meV the two resonances A and D are seen. They are marked according to their mode of excitation. Note the different scales for N_s . The polarization splitting amounts to a factor of ~ 2.5 in N_s . This is considerably more than for any previously observed resonance. It contrasts strongly with the (110) plane signals discussed above. The Raman scattering data⁸ also show the largest relative polarization splitting in the (111) plane.

In general we conclude that there is a substantial shift of the resonance excitation with the polarization mode. The sign is that predicted for the depolarization effect. Nevertheless, its magnitude, which is so unusually large for the (111) plane and particularly small for the (110) surface, is evidence for the fact that there is in addition an excitation-dependent weighting of contributions to the inhomogeneously broadened line.

C. Temperature effects

It is known that the electron subband resonances in Si, in particular for the accumulation case, depend sensitively on T .^{9,18} For the (100) plane the N_s position of a given electron resonance will shift by typically a factor of 2 when T is varied from 4.2 to 200 K. With rising T the lines shift to lower N_s . The linewidths increase only slowly, much less than the corresponding change in the transport mobility.¹⁸

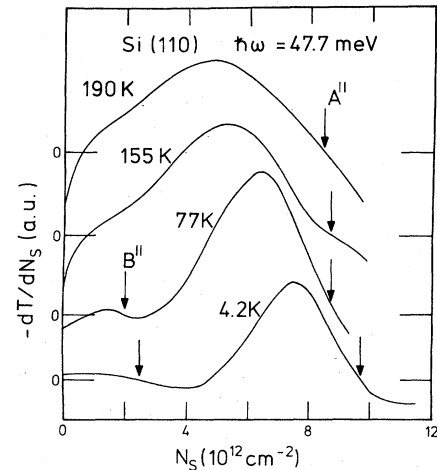


FIG. 6. Temperature shift of the resonances in the (110) plane. The shifts are small compared to those of the electron signals.

The temperature dependence for the hole resonances has been examined for each of the symmetry planes for $4.2 \leq T \leq 200$ K. Peak-position shifts to lower N_s are found with rising T , but the shifts are small. Figure 6 is a typical example for the \parallel excited (110) planes spectrum. The B^{\parallel} line moves by $\sim 10\%$ to lower N_s . The corresponding electron resonance in this plane and at this energy of excitation shifts by a factor of 2.⁹

The hole resonances in all planes are found to broaden substantially and reduce in amplitude. Thus in Fig. 6 the A can no longer be distinguished above 77 K. To the extent that hole resonances are inhomogeneously broadened, we can expect with rising T that the additional k_{\parallel} spreading of the occupied states will increase the linewidth.

The spectra in Fig. 6 are an example of the kind of signal that can be obtained with the grating spectrometer. The instrumental resolution expressed in terms of N_s is $\Delta N_s \cong 5 \times 10^{11} \text{ cm}^{-2}$.

D. Resonance spectra in the three symmetry planes

The assignment of the observed peaks to specific transitions in the scheme of the hole subbands is not at all straightforward or unambiguous. Nevertheless, our systematic observation of peak position versus $\hbar\omega$ in all the planes allows some general observations. In this discussion of the (100), (110), and (111) spectra we seek to make a plausible identification and to compare our results with the inelastic light scattering data of Ref. 8.

Starting with the (100) plane we identify the two branches A and B that are plotted in Fig. 7. Of these, the A resonance is the signal that has been reported in much of the previous work.²⁻⁵ It is observed with distinct polarization splitting. In making the switch from the laser spectrometer to the continuous frequency grating spectrometer, we have a frequency gap from 30 to 36.5 meV. The rapid drop of the grating spectrometer sensitivity makes it impossible to follow the A resonance from high frequencies to the 30.2-meV point continuously. In spite

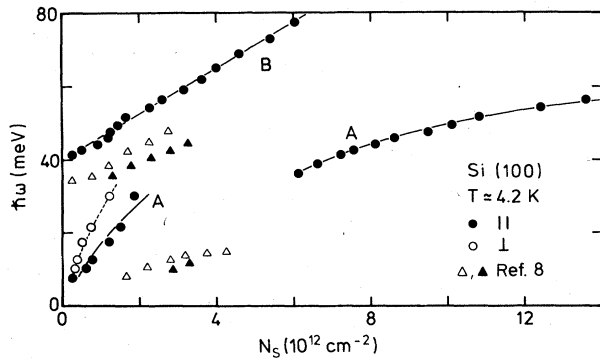


FIG. 7. Absorption maxima A and B as observed in the (100) plane for the \perp and \parallel polarization modes. For instrumental reasons the \perp mode is observed only to 30.2 meV. The open (\perp) and solid (\parallel) triangles mark signals observed in Raman experiments (Ref. 8).

of the apparent knee in the $\hbar\omega$ vs N_s relation, we believe that it is the same transition signal.

The most heavily populated subband is h_0 and one should expect that transitions in the same band are dominant (compare Fig. 1). This leads us to suggest that A represents $h_0 \rightarrow h_1$ transitions. It is not clear where in the k_{\parallel} distribution of transition energies the absorption maximum is located. The A^{\parallel} signal is also observed in Ref. 7 between 20 and 38 meV. The present data extends the spectral range. We do not resolve the weak additional structure marked in Ref. 7 as a separate branch below the A^{\parallel} line.

When $\hbar\omega > 40$ meV we identify in the (100) plane a branch labeled B . This signal has not previously been observed. The extrapolation of B^{\parallel} to $N_s \rightarrow 0$ for accumulation indicates ~ 40 meV. This identifies it unambiguously as linked to the excitation from h_0 to s_0 , the lowest subband formed from the spin-orbit-split volume band.

Turning in Fig. 8 to the (110) plane we identify the B signal from its extrapolation to $N_s = 0$. The B^{\parallel} branch rises more steeply with N_s in this plane than in the (100).

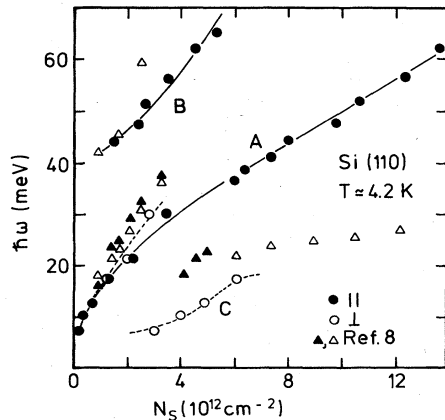


FIG. 8. Absorption maxima in the (110) plane. Branch C is not found at 21.8 meV or above and is observed as a strong signal in the \perp mode only. Triangles mark the Raman data (Ref. 8).

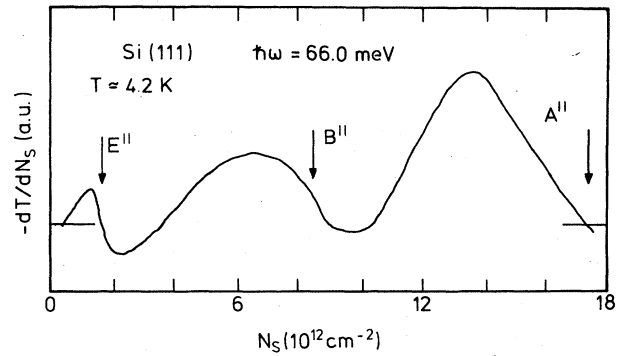


FIG. 9. Resonances A , B , and E as observed in \parallel polarization with the grating spectrometer for $\hbar\omega = 66.0$ meV.

There is observed a branch in the (110) plane which has the general characteristics of the (100) plane A signal. We speculate that it is the same $h_0 \rightarrow h_1$ transition and have labeled it accordingly as A . A third branch labeled C is found as a big signal in \perp excitation for energies between 7.2 and 17.6 meV. It is not observed at 21.7 meV and above. A possible assignment is as a transition from occupied l_0 states to h_1 . In Ref. 7 branch A is observed between 18 and 50 meV. A weak signal in parallel excita-

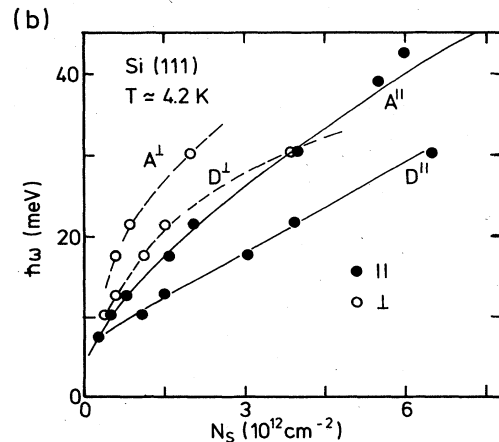
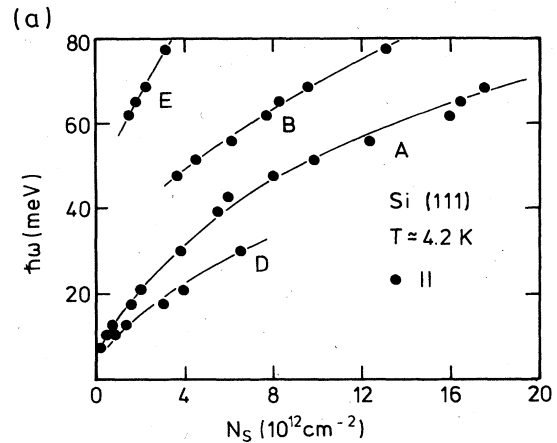


FIG. 10. (a) and (b) Absorption maxima in the (111) plane. To clearly distinguish the \perp and \parallel excitation data for low energies, an expanded scale is used in (b).

tion that relates to C^\perp is plotted in Ref. 7. No mention is made of B .

The most complex set of signals is found for the (111) plane. For high energies we identify the three peaks in Fig. 9. Of these the peaks B^\parallel and A^\parallel belong to the respective branches in Fig. 10 and should be compared with the corresponding signals in the (100) and (110) planes. Signal E^\parallel is a new transition not seen in the previously discussed planes. A possible assignment is $h_0 \rightarrow h_2$. The D branch in Fig. 10 could represent $h_0 \rightarrow l_0$ transitions. This signal looks quite different from the C signal in the (110) plane.

Comparing with Ref. 7 we note that branches A , D , and E in the parallel mode coincide where the spectral ranges overlap. We believe the B signal has been missed in that work, because of the lack of a suitable detector in the relevant energy range.

Considering the experimental uncertainties and the "in principle" problems in the identification of an absorption peak in the hole spectrum, the transition assignments relate reasonably to the energies calculated.^{8,11} Qualitative trends are well reproduced. With some account for the differences in the depletion field between calculation and experiment, one can talk of rough numerical agreement. The essential problem in relating theory and experiment is the question of what to compare. For the electron resonances the \perp excited data, because of a near cancellation of the depolarization and exciton shifts, are usually compared with the "pure" subband energy.¹⁹ For the holes there is the problem with the k_\parallel -dependent energy separations and the weighting according to the polarization mode. The experimental work on holes has concentrated on \parallel excitation.

The contrast of the inelastic-light-scattering results⁸ with the infrared spectra is striking. For most of the signal branches discussed in Figs. 7, 8, and 10 there is no corresponding Raman signal. There is, with all respect for possible experimental uncertainties, systematic disagreement. It appears that the observation precludes its observation in the other. To emphasize this situation we have in Figs. 7 and 8 entered the experimental points of Ref. 8. For the (111) plane data the Raman data points

fall within the range where the A branch is observed and thus cannot be clearly distinguished. For this reason they have been omitted from Fig. 10.

V. CONCLUDING REMARKS AND SUMMARY

We have in a series of experiments explored hole inter-subband resonances in the major symmetry planes of Si. Up to energies of ~ 30 meV data have been obtained in both polarization modes and show the splitting expected from a depolarization effect. The sign of the splitting is correct, but the large magnitude of the effect for the (100) and (111) planes suggests that the splitting is not purely a consequence of depolarization.

The contrast with the Raman results suggests that the two experiments basically measure something else. This is a surprising realization that should stimulate further thoughts. The Raman excitation experiments involve different matrix elements, so that amplitudes and observabilities may vary between Raman and ir. In addition, the k_\parallel dependence of transition energies is expected to influence the peak position. This could account for the different energy values observed in the two experiments. Many-body effects, such as the exciton shift, could appear in another way in the Raman and ir measurements.

In each of the three surfaces the resonances follow a general pattern. There is a branch at high energy which extrapolates to ~ 40 meV of energy for $N_s \rightarrow 0$. For obvious reasons this B signal has been assigned to $h_0 \rightarrow s_0$ transitions. The dominant A peak at intermediate energies and extrapolating to zero for $N_s = 0$ in accumulation has been assigned as a $h_0 \rightarrow h_1$ transition. It also is found in all planes. The lowest transition-energy branch varies from plane to plane. In the (111) plane its extrapolation suggests a $h_0 \rightarrow l_0$ transition. For (110) it appears to be a transition from an occupied l_0 state to h_1 .

We conclude that some understanding of the hole spectra has been gained, but that knowledge of significant details will require additional calculations. What is needed is a calculation that takes proper account of the experimental conditions.

¹T. Ando, A. B. Fowler, and F. Stern, *Rev. Mod. Phys.* **54**, 437 (1982).

²A. Kamgar, P. Kneschaurek, W. Beinvogl, and F. Koch, in *Proceedings of the 12th International Conference on the Physics of Semiconductors*, edited by M. H. Pilkuhn (Teubner, Stuttgart, 1974), p. 709.

³P. Kneschaurek, A. Kamgar, and F. Koch, *Phys. Rev. B* **14**, 1610 (1976).

⁴A. Kamgar, *Solid State Commun.* **21**, 823 (1977).

⁵U. Claessen, diploma thesis, Technical University München, 1981 (unpublished).

⁶A. D. Wieck, E. Batke, D. Heitmann, and J. P. Kotthaus, *Surf. Sci.* **142**, 442 (1984).

⁷A. D. Wieck, E. Batke, D. Heitmann, and J. P. Kotthaus, *Phys. Rev. B* **30**, 4653 (1984).

⁸M. Baumgartner, G. Abstreiter, and E. Bangert, *J. Phys. C* **17**, 1617 (1984).

⁹Soe-Mie Nee, U. Claessen, and F. Koch, *Phys. Rev. B* **29**, 3449 (1984).

¹⁰F. J. Ohkawa and Y. Uemura, *Suppl. Prog. Theor. Phys.* **57**, 164 (1975).

¹¹E. Bangert (unpublished), and private communication.

¹²F. J. Ohkawa, *J. Phys. Soc. Jpn.* **41**, 122 (1976).

¹³W. Zawadzki, *J. Phys. C* **16**, 229 (1983).

¹⁴K. Wiesinger, H. Reisinger, and F. Koch, *Surf. Sci.* **113**, 102 (1982).

¹⁵F. Martelli, C. Mazuré, and F. Koch, *Solid State Commun.* **49**, 505 (1984).

¹⁶T. Cole and B. D. McCombe, *Phys. Rev. B* **29**, 3180 (1984).

¹⁷A. Gold, W. Götze, C. Mazuré, and F. Koch, *Solid State Commun.* **49**, 1085 (1984).

¹⁸F. Schäffler and F. Koch, *Solid State Commun.* **37**, 365 (1981).

¹⁹T. Ando, *Z. Phys. B* **26**, 263 (1977).